

# Imaging of high current and high charge-state ion beams using a Sapphire scintillator

PS/HP Note 2000-004

*O. Camut, K. Hanke, S. Kondrashev<sup>1)</sup>, H. Kugler, C. Meyer,  
B. Pincott, G. Probert, R. Scrivens and A. Shumshurov<sup>1)</sup>*

CERN PS Division, CH-1211 Geneva 23, Switzerland

<sup>1)</sup>ITEP, Moscow, 117259, Russia

## 1- Introduction

Imaging of high current and high charge-state ion beams was conducted using a sapphire scintillator. In comparison with a phosphor screen a sapphire crystal has a damage threshold higher by several orders of magnitude and also a wider range of linearity. The Tantalum (Ta) ions were produced from a CO<sub>2</sub> laser-generated plasma. To obtain an image of the extracted ion beam a sapphire crystal disk, 78 mm in diameter and 500  $\mu\text{m}$  in thickness, was installed 15 mm after the last grid of a Gridded Electrostatic Lens (GEL) focusing system. A mesh was placed in front of the sapphire surface so that a potential could be applied and static potential at the crystal surface avoided. This would allow variation of the secondary electron emission current. Two extraction voltages  $V_{\text{ext}} = 65$  and 80 kV were used during the experiment.

## 2- Experimental Setup

The experimental configuration showing the CO<sub>2</sub> laser, extraction system and focusing system is displayed in Figure 1 together with the mesh and sapphire arrangement. A CCD Hadland Photonics camera and a 500 mm lens objective were used to record the images. The distance from the sapphire to the lens was set to 185 cm so that the camera could be placed outside the high voltage area. The resolution of the readout system was 9.1 pixels/mm.

## 3- Experimental Results

To investigate the strength of the sapphire crystal scintillator to high current densities the ion beam was tightly focused onto the sapphire crystal. In the data analysis, the x-ray background was removed from the real signal. Figures 2 and 3 show the focal beam distribution for two different extraction voltages  $V_{\text{ext}} = 80$  and 65 kV, respectively. The corresponding horizontal profiles are also displayed in Figures 4 and 5. From these traces the FWHM diameters for the 80 kV and 65 kV cases are found to be 5.5 and 9 mm, respectively.

A study of the variation of the beam size with respect to the last GEL electrode voltage was carried out. The experimental plot showing very well this dependence is displayed in Figure 6 together with two additional plots obtained from two simulation codes: Kobra (run in 3D and taking a Gaussian beam profile right after extraction) and Igun (run in 2D, starting from a plasma, and including the geometry of the extraction system). Both codes assume that the beam current is time independent whereas in reality the current fluctuates in time. The optics will change since the magnitude of the space charge forces is a strong function of the current. This could partly explain why a larger beam size is measured in the experiment.

Gaussian fits of image traces from ion beams extracted at 65 kV show ring-like spatial structure of the beam. The horizontal profile of Figure 7 for a 3-8  $\mu\text{s}$  integration time displays one ring around the central part of the beam, while in Figure 8 for 3-20  $\mu\text{s}$  at least two rings can be observed.

To evaluate the amount of noise coming from the x-rays a thin mylar foil was inserted between the mesh and the sapphire. This would, in principle, stop the ion beam and let the light pass through. It was found that this foil fully stopped the beam but part of the ion kinetic energy is turned into radiation emitted by the foil and hence an image of the beam could still be obtained.

Figure 9 shows an image of an ion beam between the 3-8  $\mu\text{s}$  time window with the presence of a strong background, while Figure 10 shows an image of the ion beam between the 15-20  $\mu\text{s}$  time window with a background close to zero.

Finally, an image of the background for different delay times (3-15  $\mu\text{s}$ ) with a gate of 3  $\mu\text{s}$  was obtained by switching off both the extraction and the GEL voltages. A constant decrease of the light intensity was observed. This demonstrates that the background subtracted during the data analysis within the time window of interest (3-8  $\mu\text{s}$ ) comes exclusively from the light emitted throughout the laser-target interaction and plasma chamber walls interaction.

#### **4- Examination of the Sapphire Surface**

The surface of the crystal exposed to 105 shots was examined with an electron microscope. The average kinetic energy incident on the sapphire surface for the Ta ions was ranging between 0.065 MeV and 2 MeV for an average current density lying between 76 mA/cm<sup>2</sup> at 65 kV and 305 mA/cm<sup>2</sup> at 80 kV. Both the central part of the sapphire which was exposed to the beam and the outside part not exposed to the beam were compared as shown in Figure 11. Note that the images are about 220  $\mu\text{m}$  wide. The state of the surface is identical, with the presence of a few scratches in each case.

## 5- Conclusion

This experiment has revealed that the sapphire crystal works as a good scintillator to image intense heavy ion beams at the focal position. It has a fast recovery time and seems not to saturate at particle interaction of  $< 1.25E11$  Ta ions (60 mA,  $5 \mu s$ ,  $\langle Ta \rangle = 15+$ ,  $E/z = 65-80$  keV). However, in close proximity to the laser ion source, it suffers from its high sensitivity to the x-ray background. In the absence of such an x-ray field, the crystal would be more useful. It should be pointed out that if the lens objective is placed at a much shorter distance from the sapphire, the collected signal coming from the ion beam should be significantly enhanced and the CCD noise reduced.

## References :

See also LIS weekly report 17-19/04/2000.

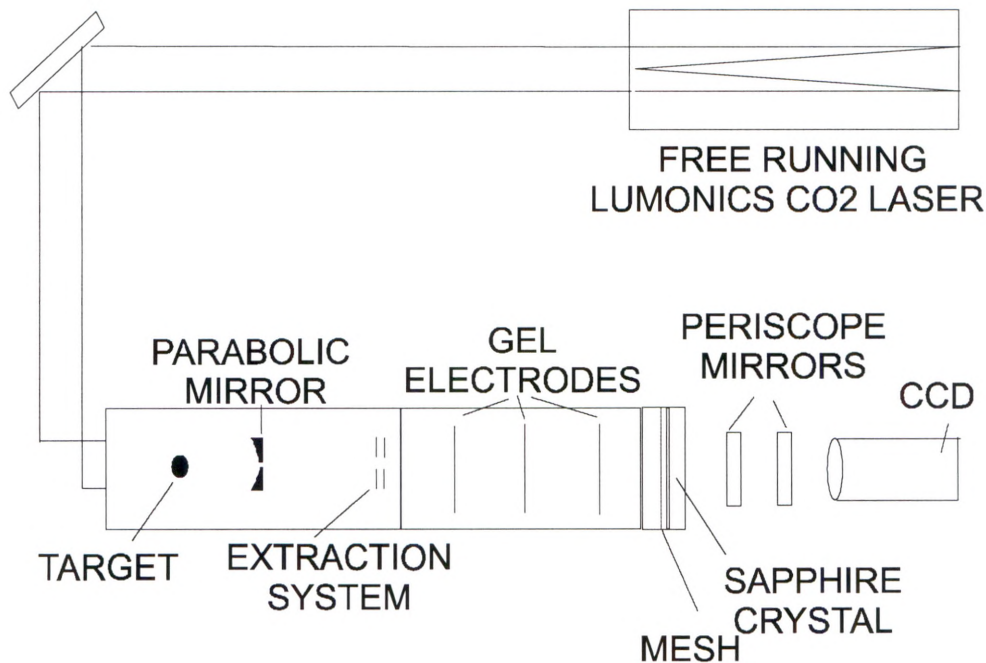


**Figure 1:** Experimental setup.

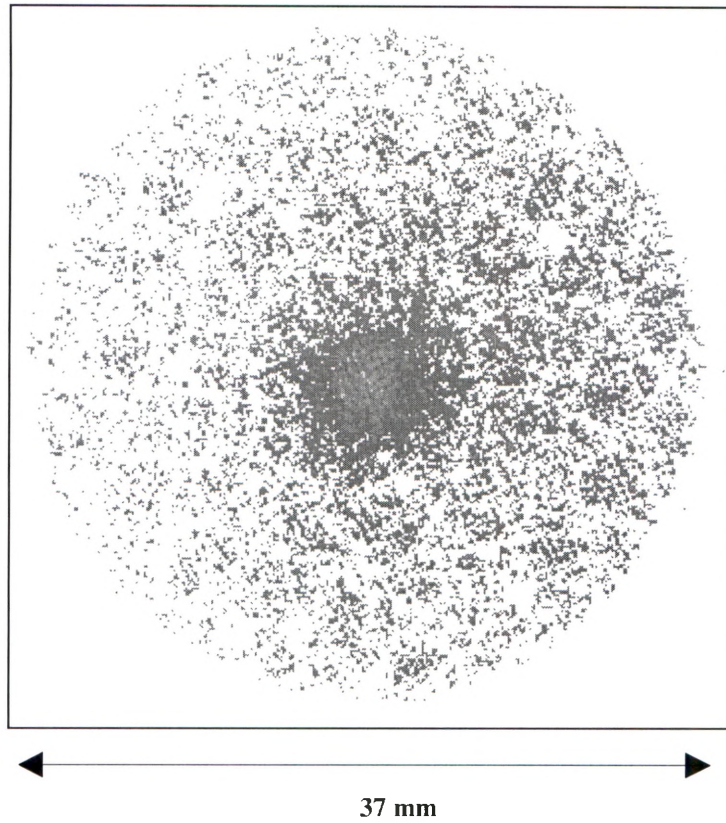


**Figure 2:** 2D image, 5  $\mu$ s gate, 80 kV extraction, 10,40,45 kV GEL and +1 kV mesh bias.

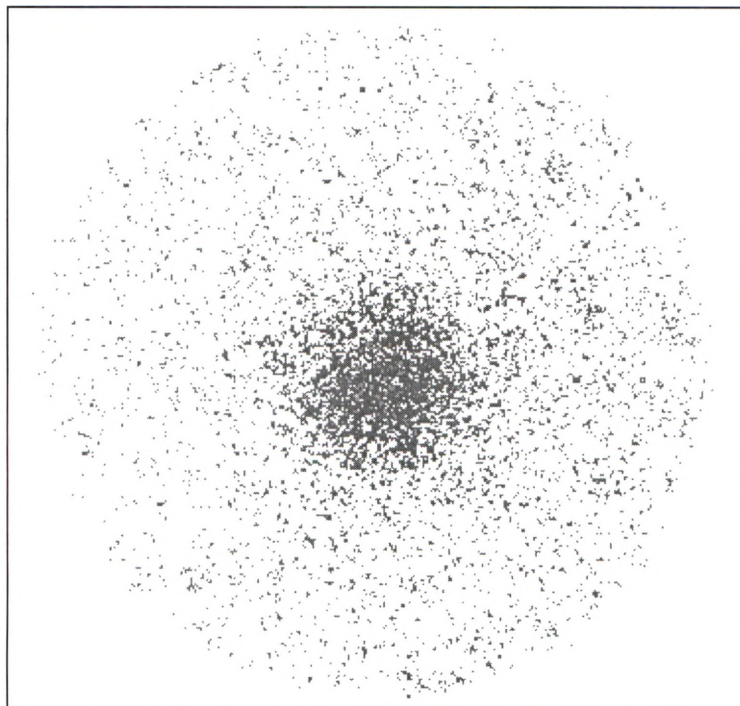


**Figure 3:** 2D image, 5  $\mu$ s gate, 65 kV extraction, 7.6, 34.7, 22 kV GEL and +500 V mesh bias. Image averaged over 8 shots with average background subtracted.

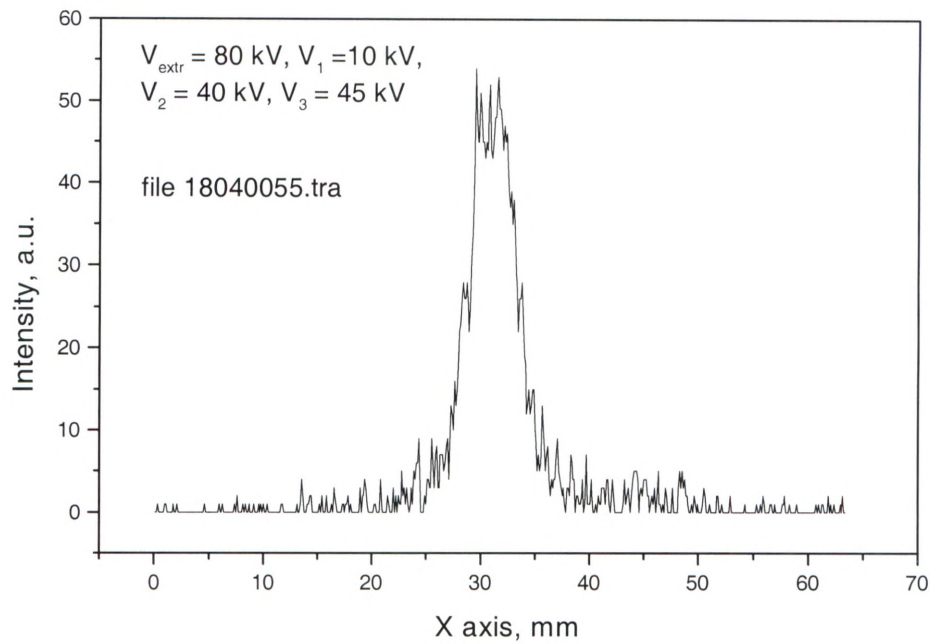


**Figure 4:** Horizontal profile,  $5 \mu\text{s}$  gate, 80 kV extraction, 10,40,45 kV GEL and +1 kV mesh bias. The FWHM beam diameter is 5.5 mm.

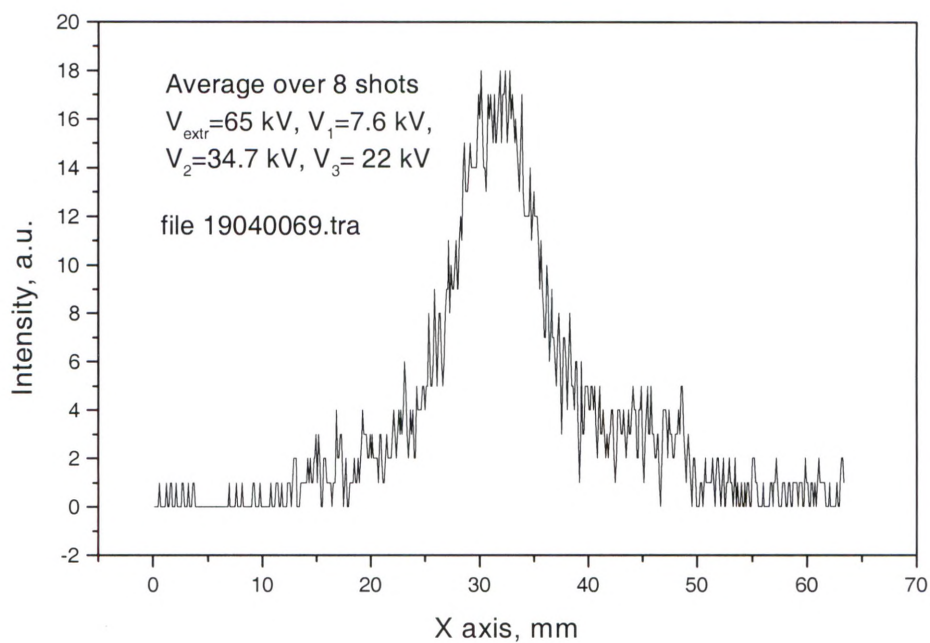


**Figure 5:** Horizontal profile,  $5 \mu\text{s}$  gate, 65 kV extraction, 7.6, 34.7, 22 kV GEL and +500 V mesh bias. The FWHM beam diameter is 9 mm.



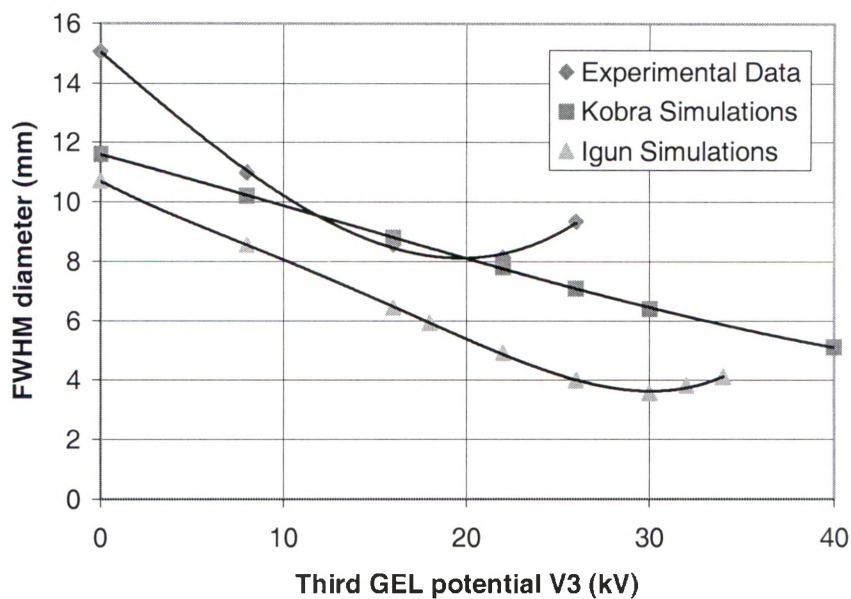


**Figure 6:** Variation of the beam size after the GEL from the experiment and the simulations,  $V_{\text{ext}} = 65$  kV,  $V_1 = 7.6$  kV and  $V_2 = 34.7$  kV.

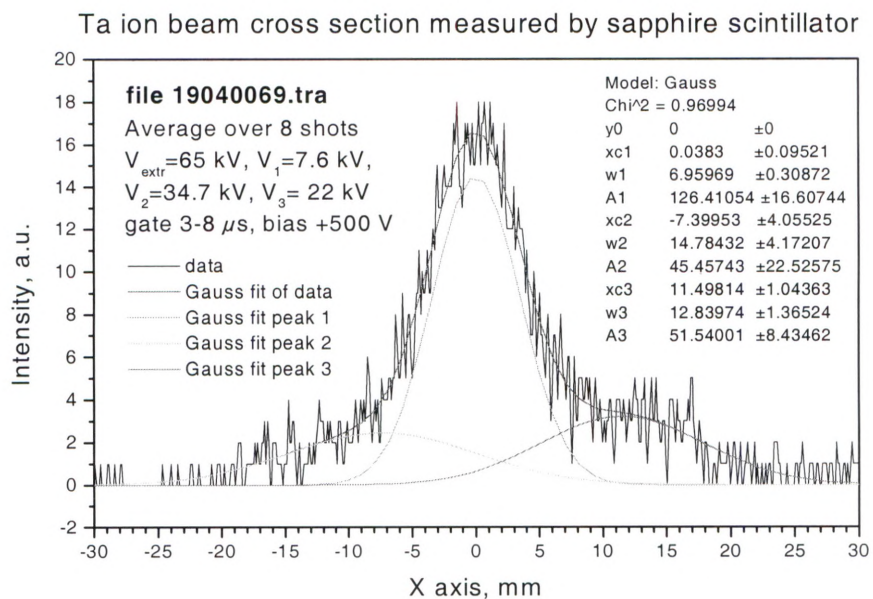


**Figure 7:** Horizontal profile, 3-8  $\mu\text{s}$  gating, 65 kV extraction, 7.6, 34.7, 22 kV GEL and +500 V mesh bias.

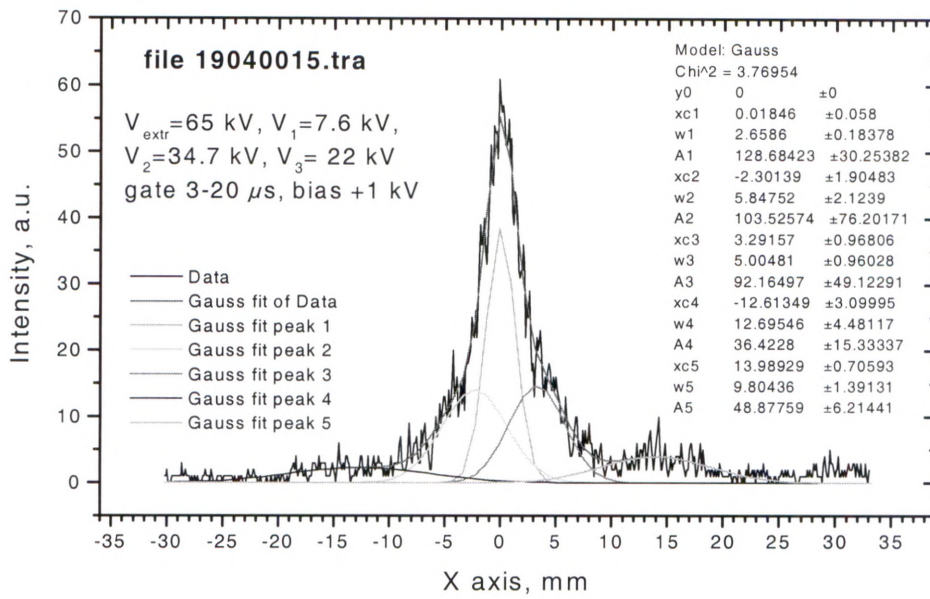


**Figure 8:** Horizontal profile, 3-20  $\mu\text{s}$  gating, 65 kV extraction, 7.6, 34.7, 22 kV GEL and +1 kV mesh bias.

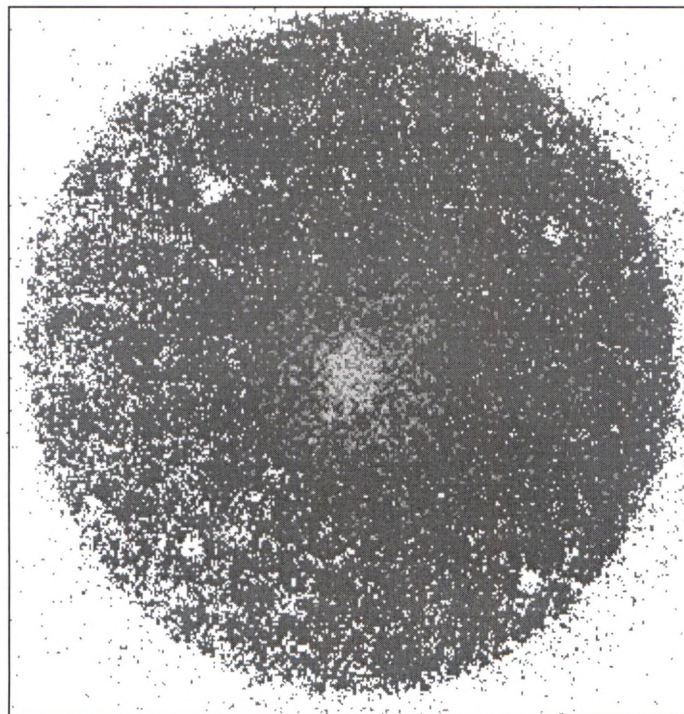


**Figure 9:** 2D image, 3-8  $\mu\text{s}$  gating, 65 kV extraction, 7.6, 34.7, 22 kV GEL and +1 kV mesh bias.

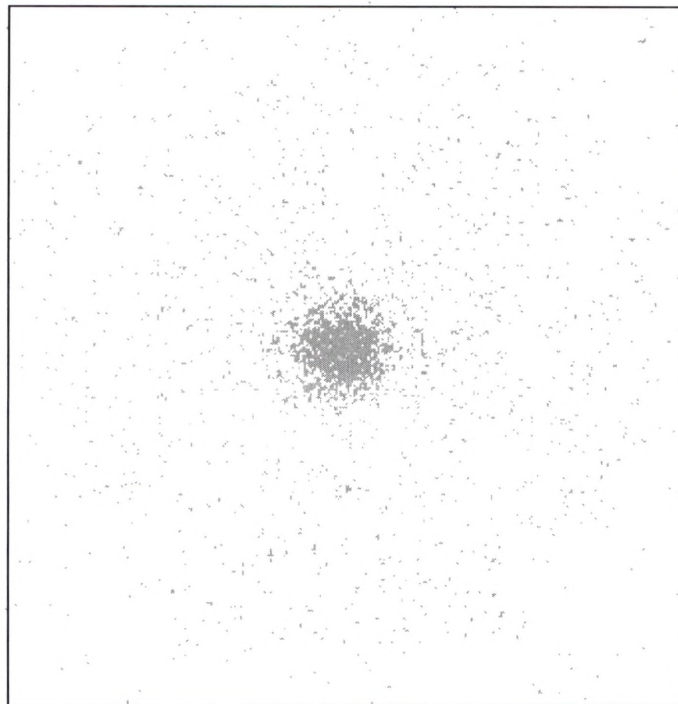


**Figure 10:** 2D image, 15-20  $\mu$ s gating, 65 kV extraction, 7.6, 34.7, 22 kV GEL and +1 kV mesh bias.



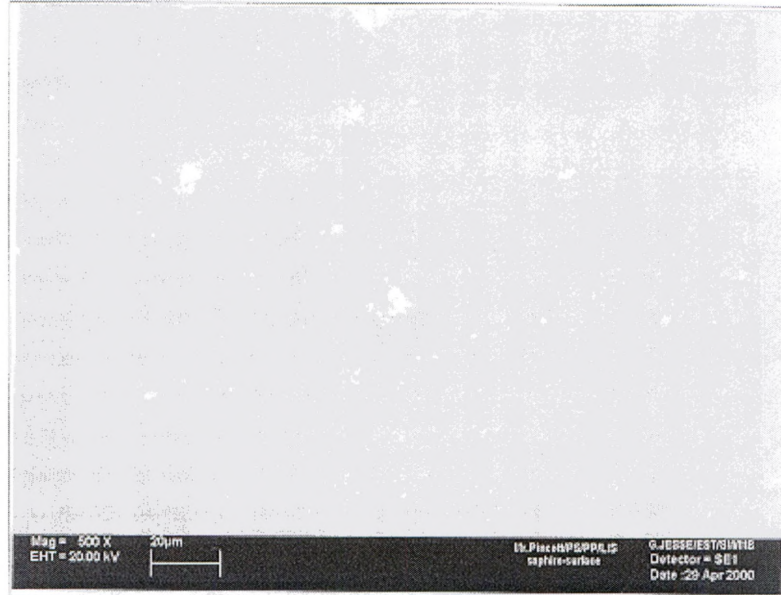


Photo No.1 - surface du saphir vers l'extérieur

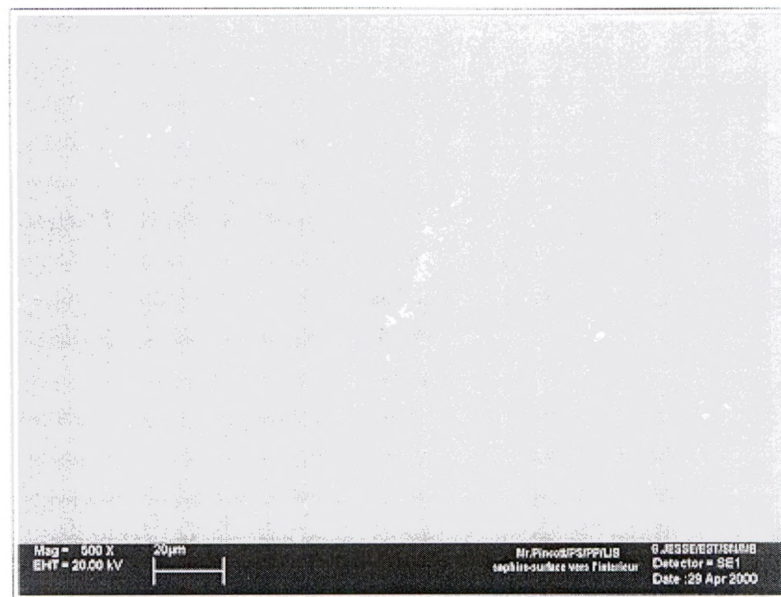


Photo No.2 - surface du saphir milieu

**Figure 11:** The top picture corresponds to the outside part (not exposed) while the bottom picture represents the central part (exposed) of the sapphire crystal.